Enhancement Progress Meeting

2026 Design of Compact Neutron Spectrometer for JT-60SA

D. Rigamonti[1] , F. Scioscioli[1], M. Cecconello[2] on behalf of the WPSA Enhancement neutron team[1, 2, 3, 4, 5, 6, 7, 8]

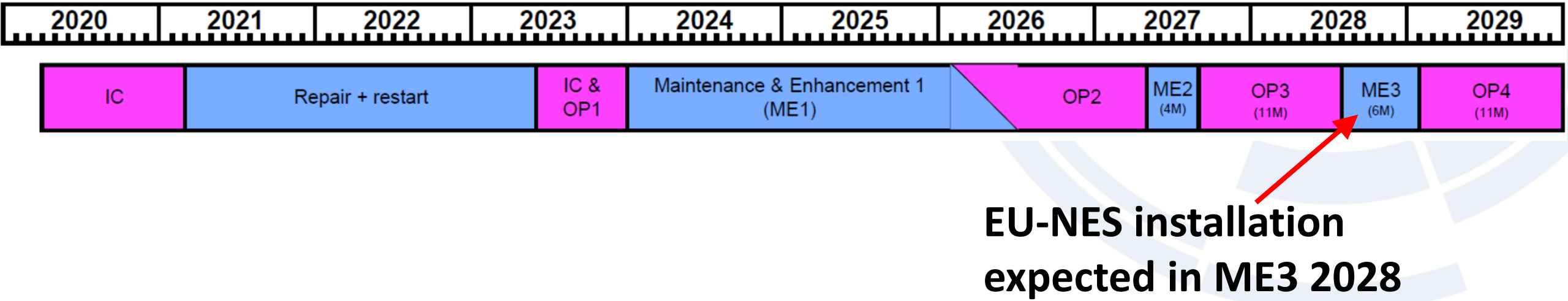
[1]Institute for Plasma Science and Technology, National Research Council of Italy, Milan, Italy
[2]Department of Physics and Astronomy, Uppsala University, Sweden
[3]National Centre for Nuclear Research, A. Sołtana 7 str., 05-400, Otwock-Świerk, Poland
[4]Department of Physics, University of Milano-Bicocca, Milan, Italy
[5]Fusion for Energy - F4E 85748 Garching, Germany
[6]Department of Mechanical Engineering and Manufacturing, University of Seville, Spain
[7]Graduate School of Engineering, Nagoya University, Furo-cho, Chikusa-ku, Nagoya 464-8603, Japan
[8]Naka Institute for Fusion Science and Technology, National Institutes for Quantum Science and Technology, Naka, Ibaraki 311-0193, Japan

This work has been carried out within the framework of the EUROfusion Consortium, funded by the European Union via the Euratom Research and Training Programme (Grant Agreement No 101052200 — EUROfusion). Views and opinions expressed are however those of the author(s) only and do not necessarily reflect those of the European Union or the European Commission. Neither the European Union nor the European Commission can be held responsible for them.

JT-60SA was jointly constructed and is jointly funded and exploited under the Broader Approach Agreement between Japan and EURATOM.

2026 Design of Compact Neutron Spectrometer (EU-NES) for JT-60SA

- Task description: Design a Compact Neutron Spectrometer (NES) based on LaCl3 scintillator coupled to a photomultiplier tube to be installed in the shared neutron shielding in P12.
- Activities on:
  - Design of the detector
  - Assessment of detector performances
  - Definition of preliminary interface assessment

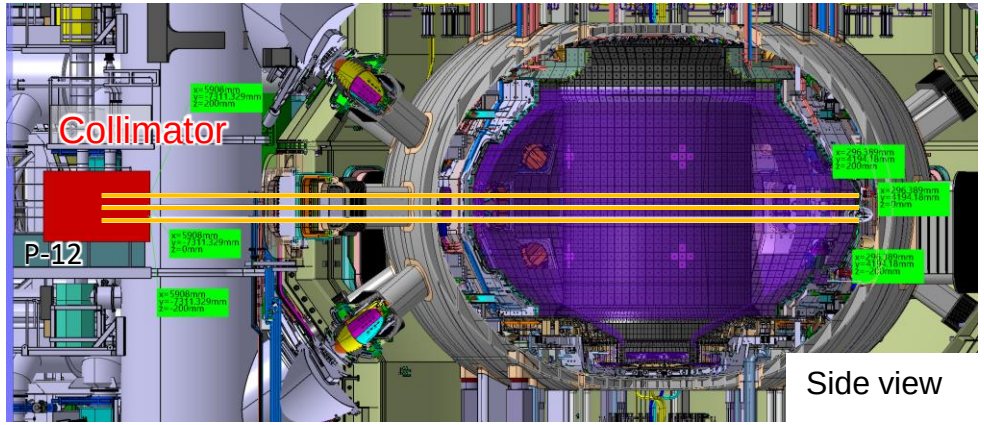


EU-NES installation expected in ME3 2028

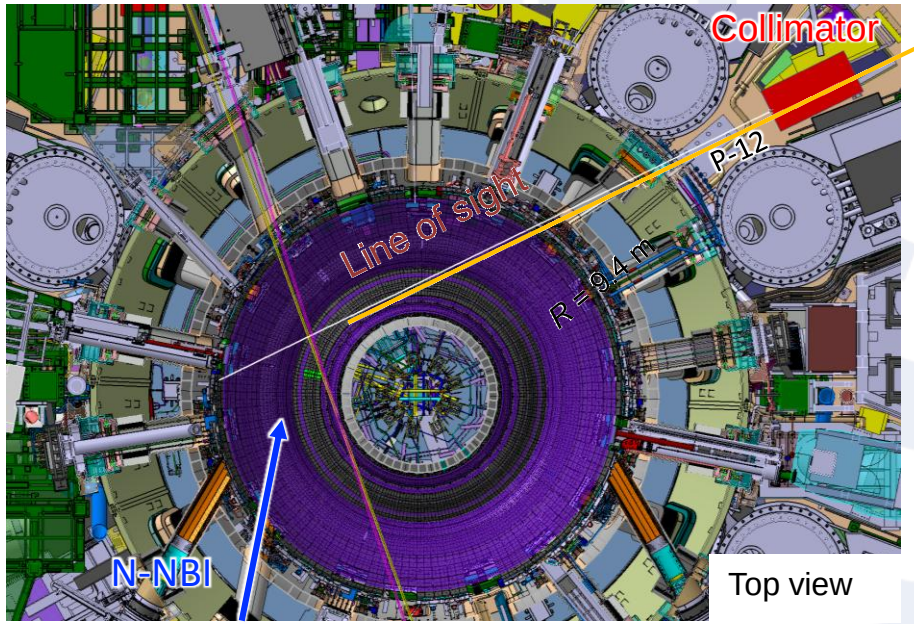
Status and plan

Current status: Detector location identified in the shared collimator in P12. The technology composing the diagnostic defined. Assessments on the magnetic shielding of the diagnostic defined. Neutron fluxes (from Uppsala team) and count rate at the detectors assessed. Detector design has been carried out considering the use of 2 interchangeable collimators.

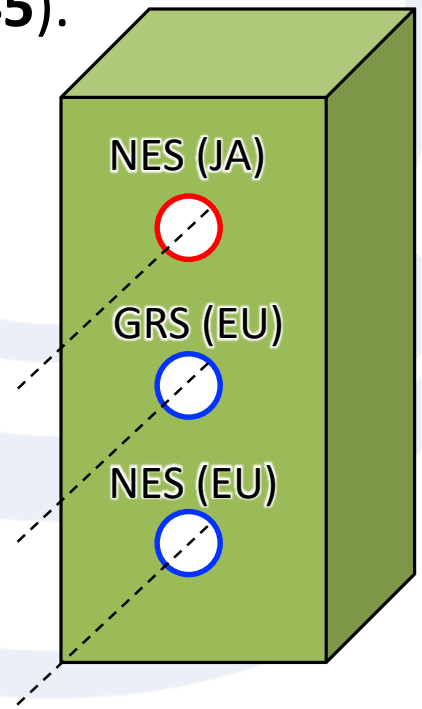
Future activity: Confirm the expected fluxes after **standardizing the sources** and definitions to ensure that the results are always comparable (**as discussed in the TCM-45**).



Side view



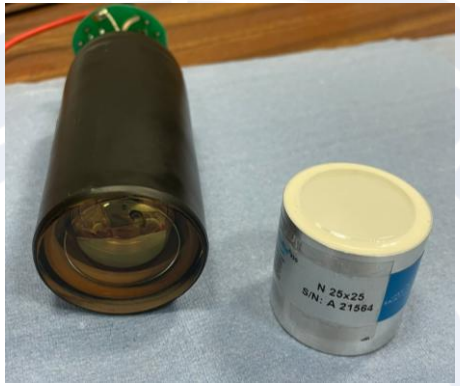
Top view



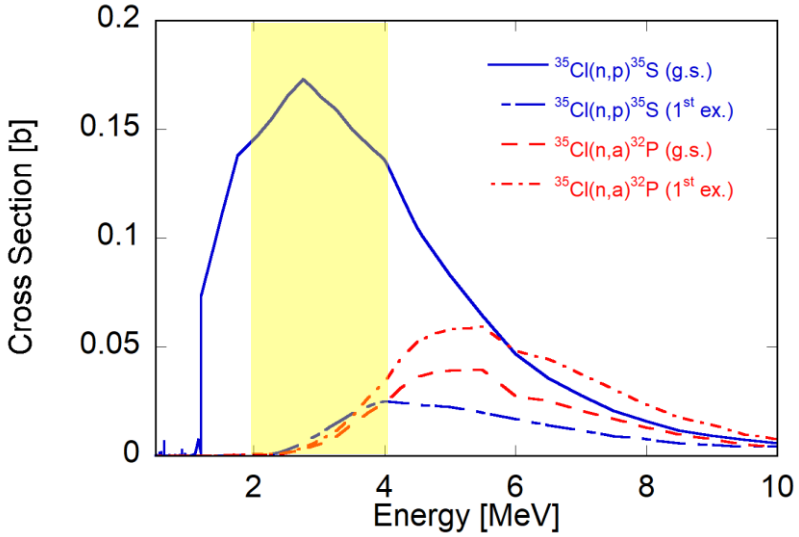
Images from Shuhei Sumida's presentation.

Lanthanum Chlorine $LaCl_3$ scintillators

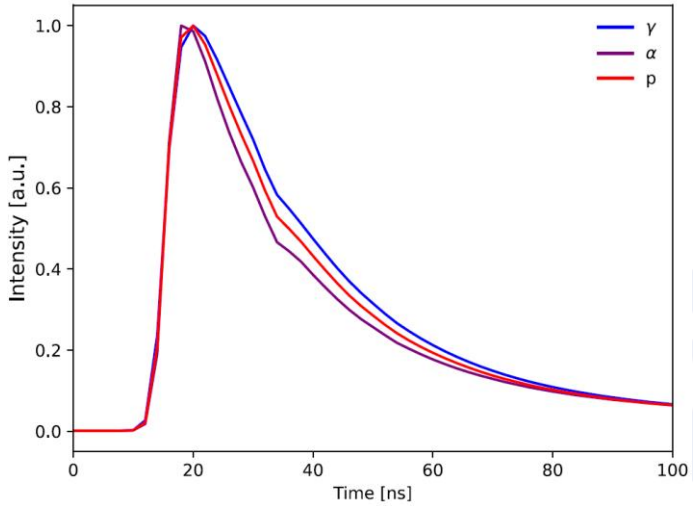
- In $LaCl_3$ neutron detection is possible thanks to the n-p reactions with ^{35}Cl (but other reactions can occur)
- **High energy resolution (49000 ph/MeV)**
- **Fast scintillation (28 ns) -> enabling measurements at count rates**
- **n/γ discrimination with enhanced algorithm**



Picture of a PMT and a $LaCl_3$ scintillator.



n-^{35}Cl cross sections.

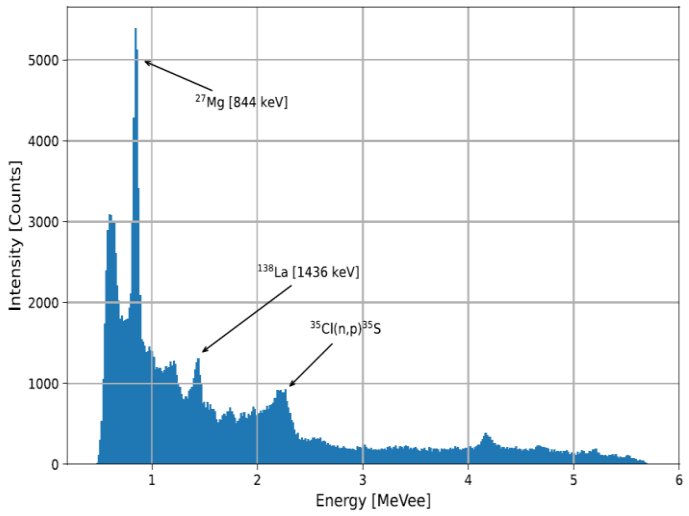


Waveforms in time domain.

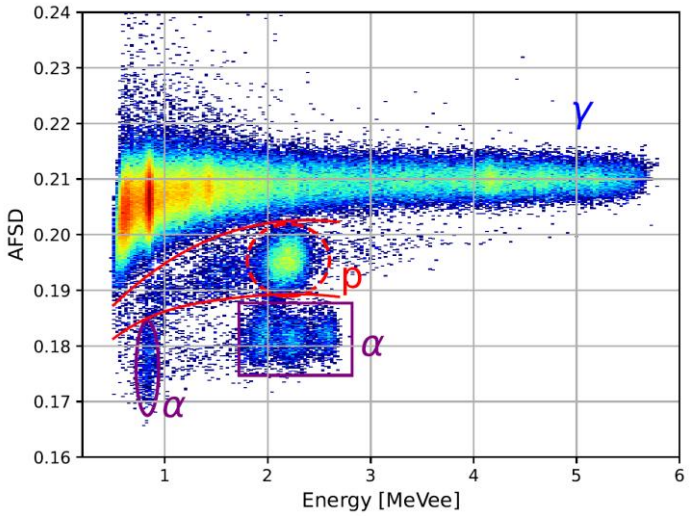
Spectroscopic measurements of 2.5 MeV neutrons with a compact instrument are now possible!

Particle discrimination

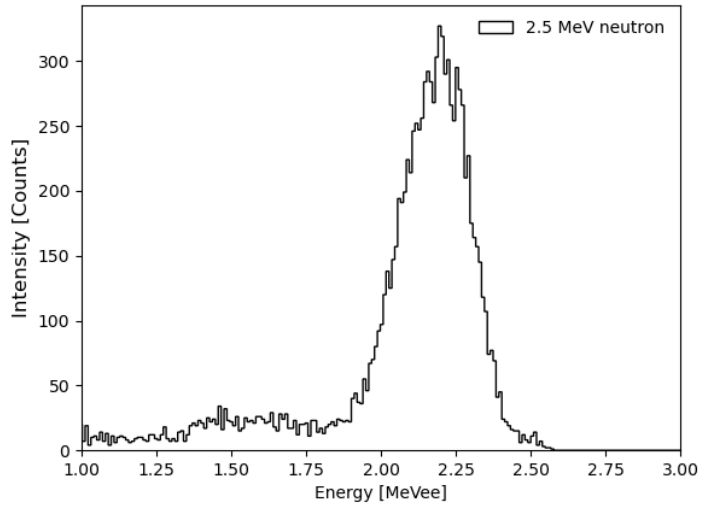
- Standard Pulse Shape Discrimination (PSD) not working properly
- New method based on **Fast Fourier Transforms FFT** has been developed and tested with **intrinsic activity** measurements (**γ and α events**) of the $LaCl_3$ crystal itself and then with **neutrons**.



Total energy spectrum measured with $LaCl_3$ base detector during 2.5 MeV neutron irradiation.



2D scatterplot for particle discrimination.

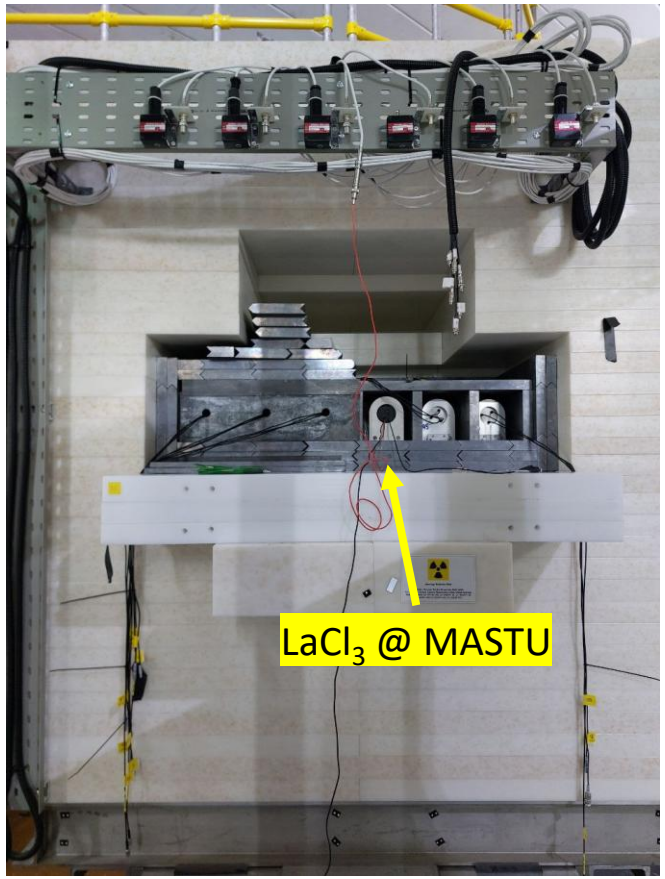


Proton peak representative of the 2.5 MeV neutrons after particle discrimination.

D Rigamonti et al 2025 Meas. Sci. Technol. 36 015907
D Rigamonti et al 2026 Meas. Sci. Technol. 37 065501

LaCl3 experience on tokamaks

- Detector design is based on the recent installations done at MAST-U, ASDEXu and EAST.

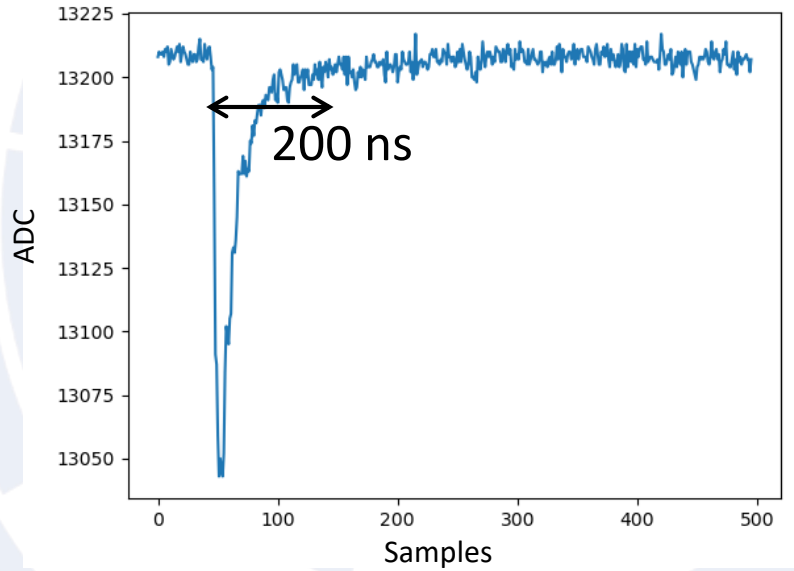


The $LaCl_3$ installed in the upgraded MAST-U neutron camera.



The $LaCl_3$ detector installed at ASDEXu (M. Nocente's project).

At MAST and EAST the detector position is similar to the one at JT-60SA: inside the tokamak hall in a shielding box. *Experience from MAST is essential.*



- No signal degradation with 90m cable
- Energy resolution preserved
- Particle discrimination preserved

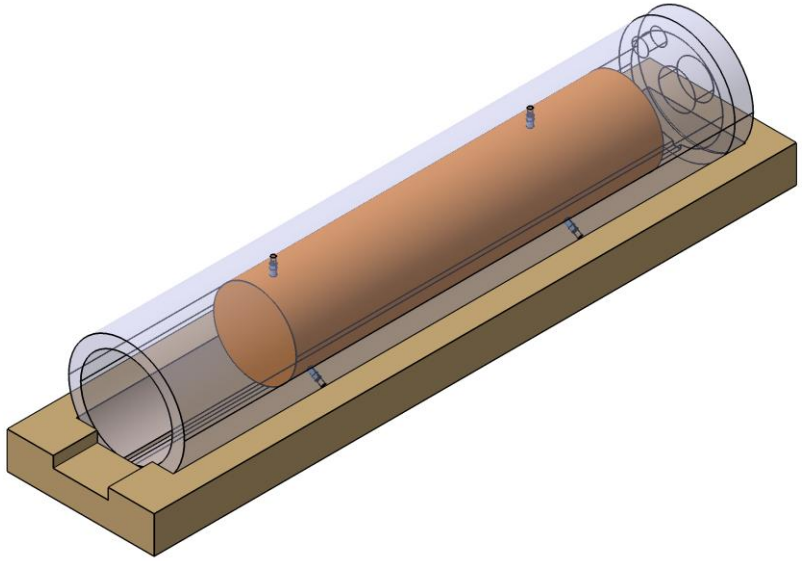
The detector design for JT-60SA

- $LaCl_3$ scintillator crystal size 10mm x 1” (diameter x height)
- PMT model R9420-100-10-Y001 made by Hamamatsu with 1.5 in nominal diameter and about 110 mm length.
- Magnetic shielding: A double shield based on 1.5 mm thick mu-metal cylinder (42 mm inner diameter and length 180 mm) and a 8 mm thick soft iron cylinder (50 mm inner diameter and length 300 mm).
- A signal cable (RG58) with BNC termination.
- A HV cable (RG58) with SHV termination.
- 0.25 mm PMMA optical fibre cable for gain stability monitor
- Electronics in PIG room (60 m) -> tests with long cables done in lab and at MAST-U
  - Digitizer* (Teledyne ADQ14DC-4C-VG-PXIe + Controller Adlink PXIe-3987 + Chassis Adlink PXIe-2301/EU3U) (sharable with GRS. TBC)
  - HV supply module* (shared with GRS)
  - LED pulser* (shared with GRS)

*** remotely controlled**

Detector design – Mechanical components

- $LaCl_3$ scintillator crystal size 10mm x 1” (diameter x height)
- PMT model R9420-100-10-Y001 made by Hamamatsu with 1.5 in nominal diameter and about 110 mm length.
- The envelope is approximately cylindrical, with maximum diameter about 44 mm and 180 mm long.



The system within the collimator structure includes the following components:

- A plastic cradle for positioning.
- A iron magnetic shield.
- The detector proper.
- An iron cap on the back.

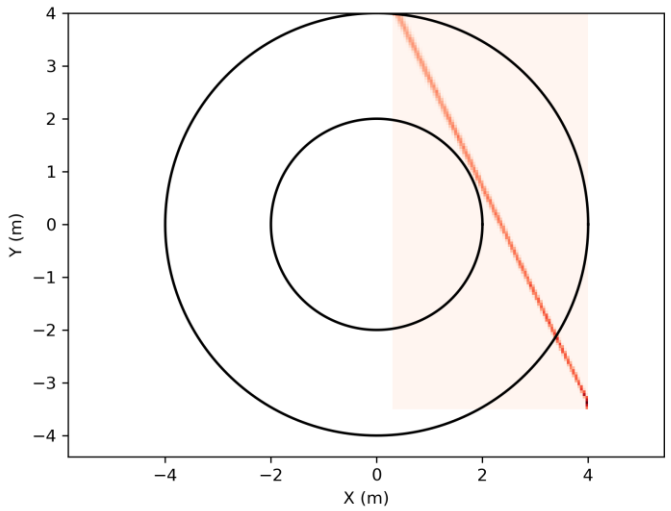
Cost estimation

Description	Model	Quantity	Estimated price (no VAT) / k€	Procurement time (m)	Comments
Crystal	LaCl3 10 mm x 1” from Luxium Solution	1	6.0	6.0	
PMT	R9420-100-10-Y001	1	1.2	6.0	Includes integration with the crystal.
Signal cable	RG58 - 100m	1	1.0	3.0	Nominal distance about 60m.
HV cable	RG58 - 100m	1	1.0	3.0	Nominal distance about 60m.
Optical fibre	PMMA	1	1.0	5.0	Nominal distance about 60m.
Other electronics	NA	1	2.0	5.0	Connectors, adapters, other cables and the like. Conservative estimate.
Magnetic shield	NA	1	1.0	3.0	The diameters are commercial.
Cradle	NA	1	0.0	0.0	Printed in-house.
Other mechanics	NA	1	1.0	3.0	Includes rear cap, screws and the like.
Collimator adapter	NA	1	2.0	3.0	Non borated HDPE. Mostly TBD, conservative estimate.
			16.2		
Digitiser	Teledyne ADQ14DC-4C-VG-PXIe	1	15.0	4.0	4 channels, may probably be shared with EU GRS.
Controller	Adlink PXIe-3987	1	7.0	4.0	May be shared with EU NES.
Chassis	Adlink PXIe-2301/EU3U	1	5.0	4.0	Compatible with JA grid. May be shared with EU NES.

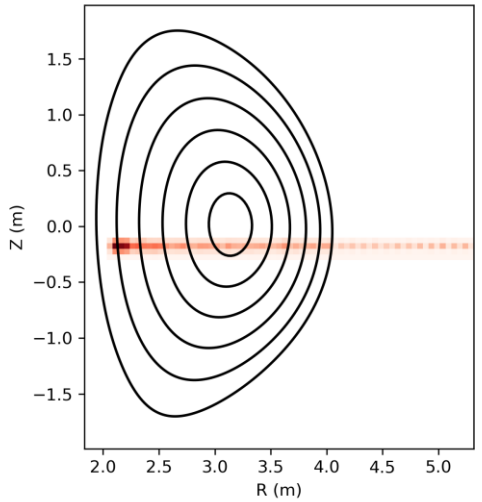
HV power supply and LED pulser shared with GRS and not included in this cost estimation

Neutron flux estimation

- The neutron flux at the detector position has been calculated with TRANSP+DRESS (Uppsala team) for scenario 2 and 5 with collimator diameter of 10 mm and 14 mm.



Top view with collimator diameter 10 mm.



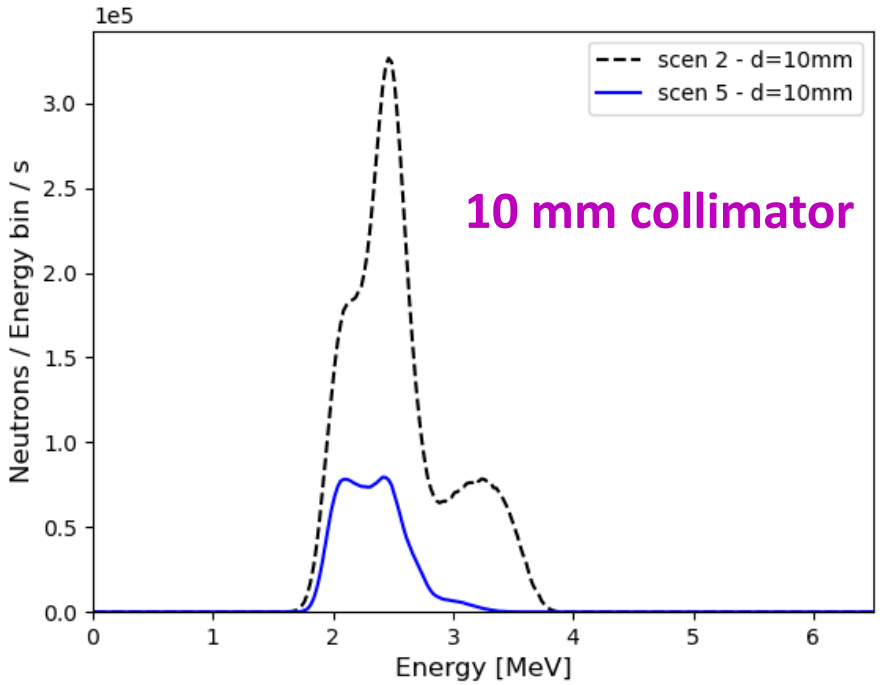
Poloidal view with collimator diameter 10 mm.

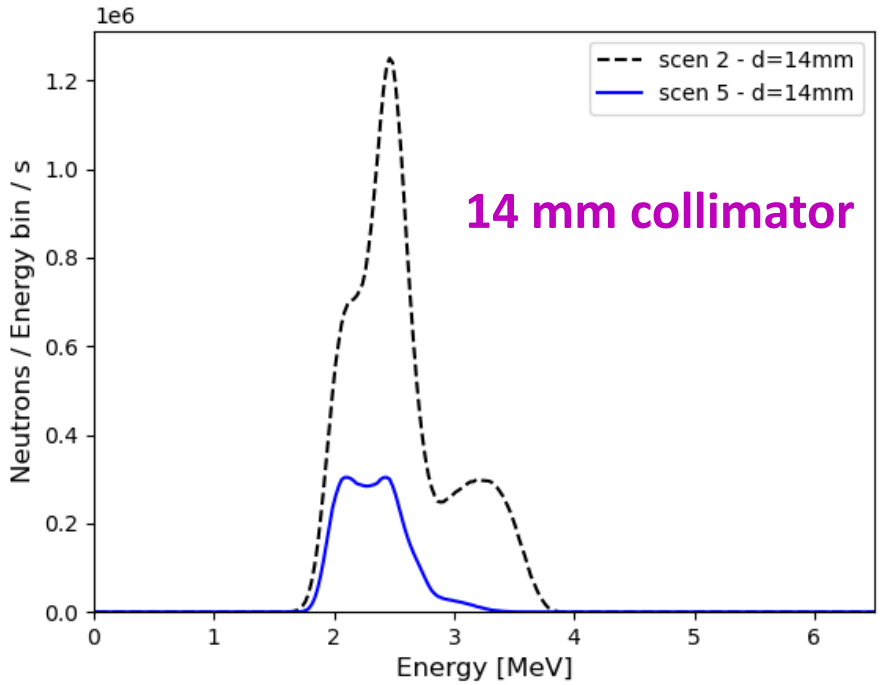
Table 3-1 Main target parameters for the typical operation scenarios with full device-capability (the order of scenario number is neither the priority nor the order of execution)

	#1	#2	#3	#4-1	#4-2	#5-1	#5-2	#6(1)
	Full Current Inductive DN, 41MW	Full Current Inductive SN, 41MW	Full Current Inductive High density	ITER-like Inductive	Advanced Inductive (hybrid)	High β_N Full-CD	High β_N High f_{GW} Full-CD	High β_N 300s
Plasma Current (MA)	5.5	5.5	5.5	4.6	3.5	2.3	2.1	2.0
Toroidal field BT (T)	2.25	2.25	2.25	2.28	2.28	1.72	1.62	1.41
q_{95}	~3	~3	~3	~3	~4.4	~5.8	6.0	~4
R/a (m/m)	2.96/1.18	2.96/1.18	2.96/1.18	2.93/1.14	2.93/1.14	2.97/1.11	2.96/1.12	2.97/1.11
Aspect ratio A	2.5	2.5	2.5	2.6	2.6	2.7	2.6	2.7
Elongation κ_x	1.95	1.87	1.86	1.81	1.80	1.90	1.91	1.91
Triangularity δ_x	0.53	0.50	0.50	0.41	0.41	0.47	0.45	0.51
Shape factor S	6.7	6.3	6.2	5.7	5.9	7.0	7.0	6.4
Volume (m^3)	132	131	131	122	122	124	124	124
Cross-section (m^2)	7.4	7.3	7.3	6.9	6.9	6.9	6.9	6.9
Normalised beta β_N	3.1	3.1	2.6	2.8	3.0	4.3	4.3	3.0
Electron density ($10^{19}m^{-3}$) Line-average/volume-average	6.3/5.6	6.3/5.6	10./9	9.1/8.1	6.9/6.2	5.0/4.2	5.3/4.3	2.0/
Greenwald density, n_{GW} ($10^{19}m^{-3}$) / f_{GW}	13/0.5	13/0.5	13/0.8	11/0.8	8.6/0.8	5.9/0.85	5.3/1.0	5.2/0.39
Plasma thermal energy, W_{TH} (MJ)	22	22	21	18	13.4	8.4	8.1	3.8
P_{add} (MW) $P_{NNB}/P_{FNB}/P_{EC}$ (MW)	41 10/24/7	41 10/24/7	30 10/20/-	34 10/24/-	37 10/20/7	37 10/20/7	30 6/17/7	13.2 3.2/6/4
Thermal confinement time, τ_{Eth} (s)	0.54	0.54	0.68	0.52	0.36	0.23	0.25	0.3
$H_{98(y,2)}$	1.3	1.3	1.1	1.1	1.2	1.3	1.38	1.3
V(V)	0.06	0.06	0.15	0.12	0.07	0	0	0.02
Resistive time (s)	34.1	32.7	16.6	15.2	14.6	12.6	10.8	12.9
Neutron production rate, S_n (n/s)	1.3×10^{17}	1.3×10^{17}	7.0×10^{16}	6.7×10^{16}	5.4×10^{16}	4.5×10^{16}	2.9×10^{16}	1.2×10^{16}

- The neutron flux has been compared with the one shown by Takeo Nishitani and Shuhei Sumida at the JT-60SA neutronics meeting of the 25th April 2025

Neutron spectra at the detector and neutron fluxes





$Yn_{TRANSP\text{-}scen2} \approx 3.5 \times 10^{17}$ n s^{-1}

$Yn_{TRANSP\text{-}scen5} \approx 7.6 \times 10^{16}$ n s^{-1}

Scenario 2

d = 10 mm -> $\phi_n \approx 1.2 \times 10^7$ n cm^{-2} s^{-1}

d = 14 mm -> $\phi_n \approx 2.4 \times 10^7$ n cm^{-2} s^{-1}

$$\phi_{n2} \propto \phi_n \cdot \frac{{d_2}^2}{{d_1}^2}$$

d = 40 mm -> $\phi_n \approx 1.9 \times 10^8$ n cm^{-2} s^{-1}

d = 80 mm -> $\phi_n \approx 7.7 \times 10^8$ n cm^{-2} s^{-1}

Scenario 5

d = 10 mm -> $\phi_n \approx 3 \times 10^6$ n cm^{-2} s^{-1}

d = 14 mm -> $\phi_n \approx 5.8 \times 10^6$ n cm^{-2} s^{-1}

d = 40 mm -> $\phi_n \approx 4.8 \times 10^7$ n cm^{-2} s^{-1}

d = 80 mm -> $\phi_n \approx 1.9 \times 10^8$ n cm^{-2} s^{-1}

Evaluation of the count rates

- The count rates for scenarios 2 and 5 were evaluated using the cross section in S. A. Kuvin et al., PRC 102, 024623 (2020). Significant discrepancy between ENDF.B and experimental data.
- Two interchangeable collimators optimized for scenario 2 or 5, respectively

Collimator diameter = 10 mm

Scenario	diameter [mm]	Length [cm]	Count rate in the peak [kHz]	"Total" count rate range [kHz]
2	10	25.4	32	640-960
5	10	25.4	9	180-275

Collimator diameter = 14 mm

Scenario	diameter [mm]	Length [cm]	Count rate in the peak [kHz]	"Total" count rate range [kHz]
2	10	25.4	79	1600-2300
5	10	25.4	18	355-550

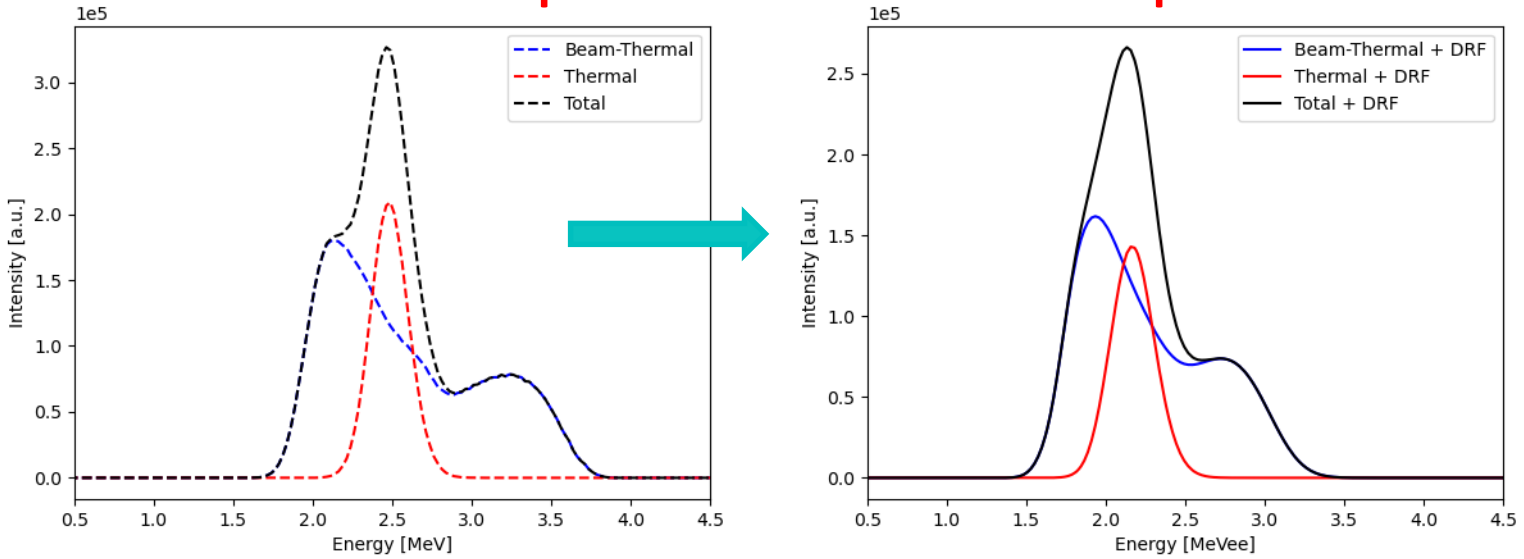
The "Total count rate" is based on previous measurements, and depends on the environment and detector size.

Neutron spectra at the detector

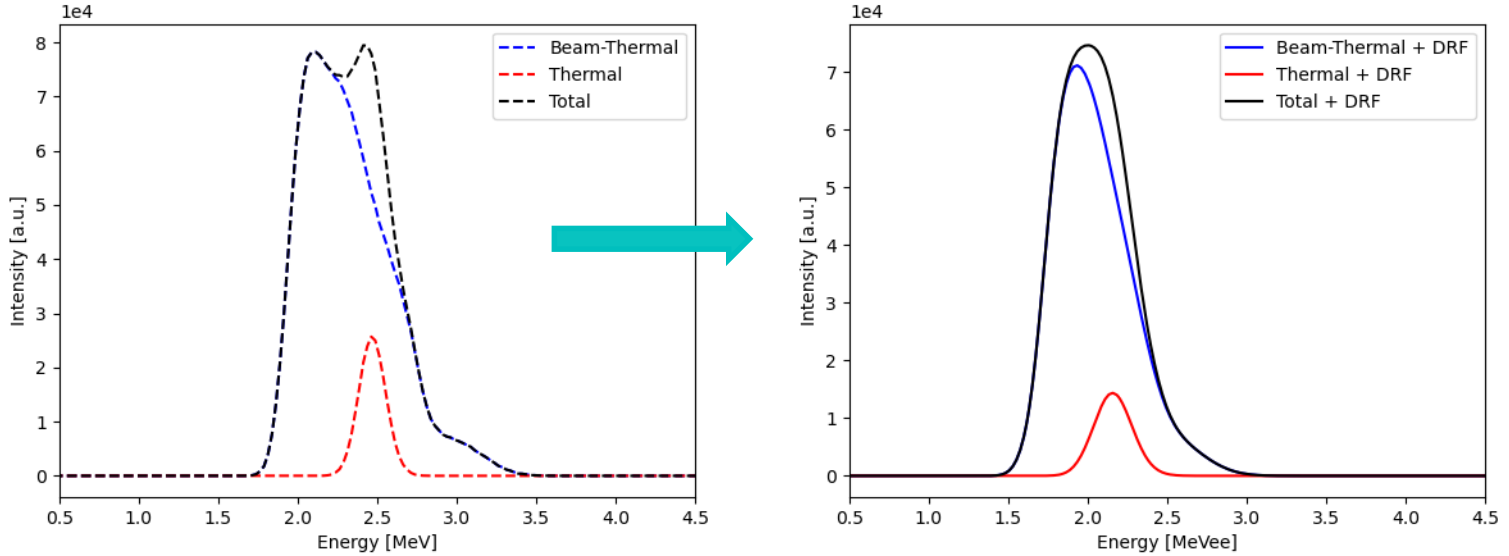
Calculated neutron spectra

Detector Response Function

Scenario 2



Scenario 5



The electron equivalent energy calculated with the empirical formula described by **Birks' law** in which the light yield of the scintillator depends on the **particle energy** and the **particle stopping power d*E*/d*x***:

$$\frac{dL}{dx} = \frac{S\frac{dE}{dx}}{1 + kB\frac{dE}{dx}}$$

dL/dx: scintillation yield density
S: scintillation efficiency
dE/dx: stopping power
kB: Birks coefficient (taken from measurements).

Conclusions

- Detector components have been identified and their costs estimated.
- Experience from other tokamaks is crucial and it has been assessed: operation at MAST-U and EAST has demonstrated that the NES is suitable for installation in the torus hall, as foreseen for JT-60SA.
- Neutron fluxes at the detector position have been calculated with TRANSP+DRESS (Uppsala team) for scenarios 2 and 5 and different collimator apertures. High neutron fluxes are expected ($\sim 10^7$ n cm^{-2} s^{-1} for a 10 mm aperture in scenario 2), constraining the detector size.
- Neutron spectra have been calculated and convolved with the detector response function (DRF).
- For the EU-NES, we propose a fixed 40 mm aperture housing interchangeable HDPE collimators (10 or 14 mm aperture), to be selected according to plasma performance.

Open points

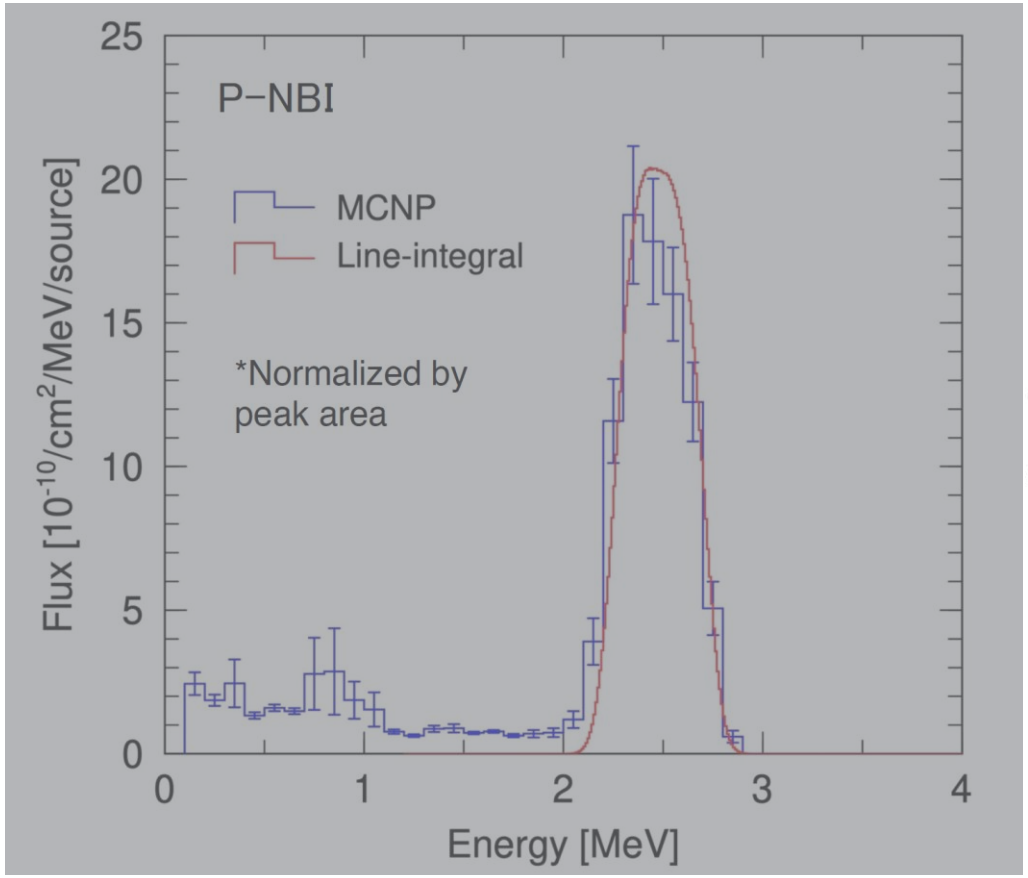
- Neutron source definitions for the different reference scenarios need to be standardized to ensure consistent and comparable results.
  - A factor of 2 discrepancy between TRANSP and Nishitani's "results", for the same total neutron yield of the plasma discharge.
  - A factor of 2 between neutron yield calculated by TRANSP and the one provided in the JT-60SA Research Plan V4.0.
- Potential interference between the EU-NES field of view and the camera needs to be assessed.
- Input from the Fast Ion Group is still needed to define the required operational dynamic range of the detector.

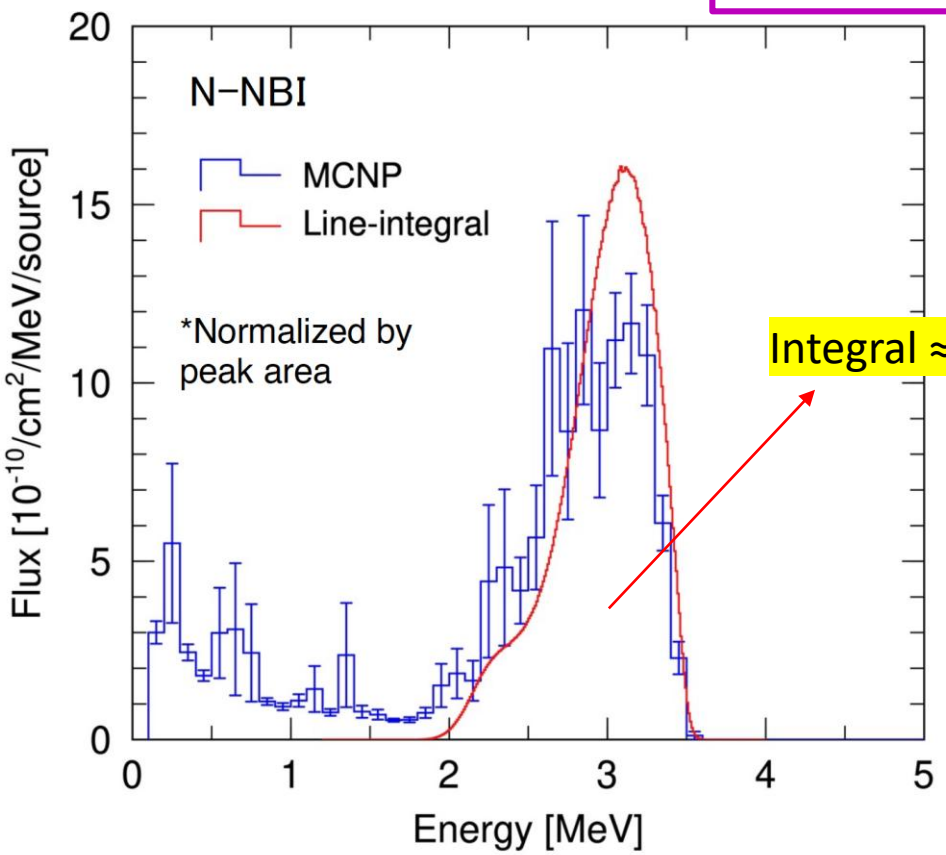
Thank you

Spare Slide

Neutron fluxes comparison with QST

Plots from Takeo Nishitani's presentation





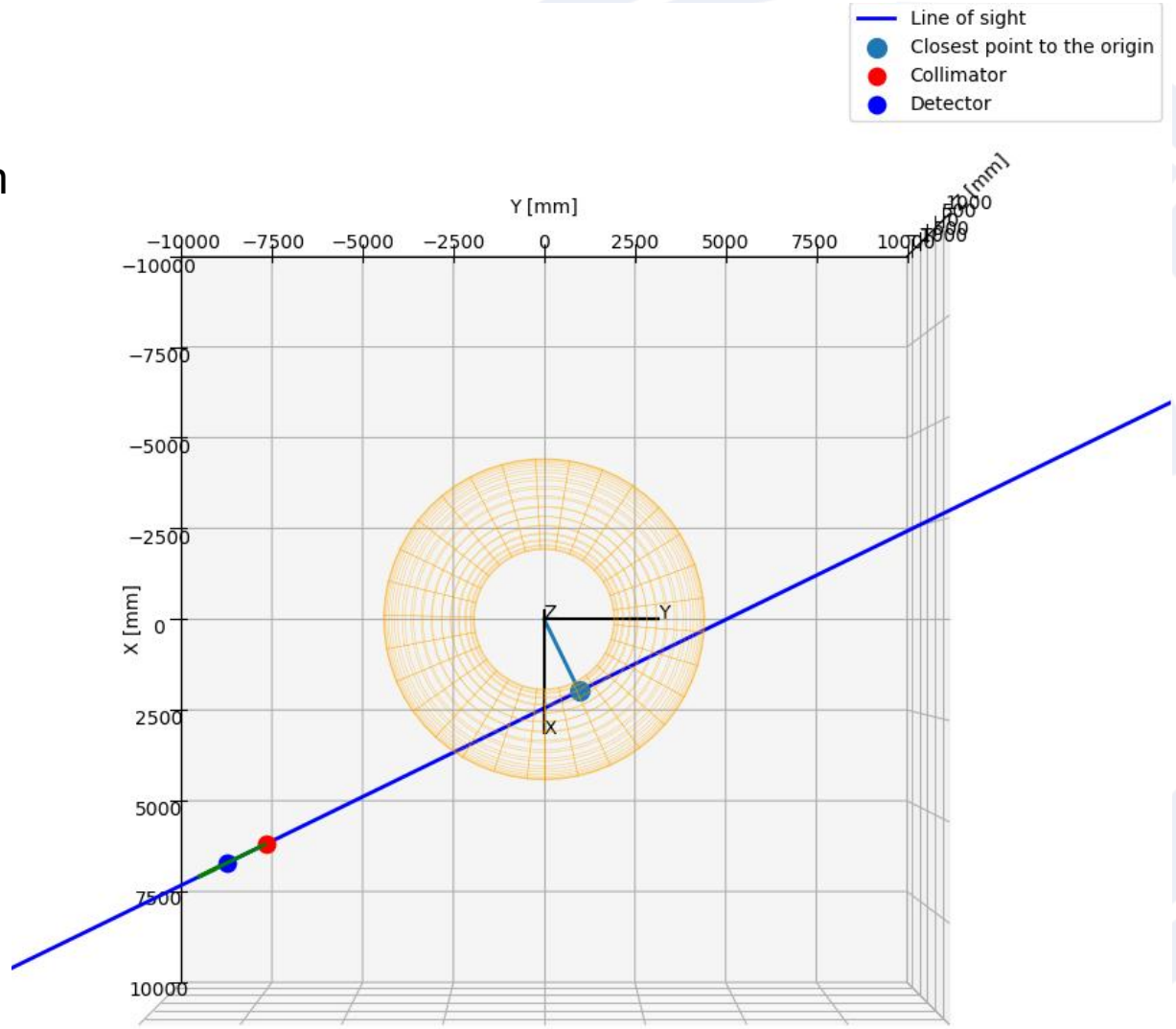
Integral ≈ 11 x 10^{-10} /cm2 / source

We assumed collimator d = 80 mm -> ϕ_n ≈ Integral x Yn_{scen2} n cm^{-2} s^{-1} -> **3.85x10^8 n cm^{-2} s^{-1}**

ϕ_n resulted to be **2 times lower** than to the one obtained with TRANSP+DRESS (7.7e8) which was specific for scenario 2. We need to understand the discrepancy.

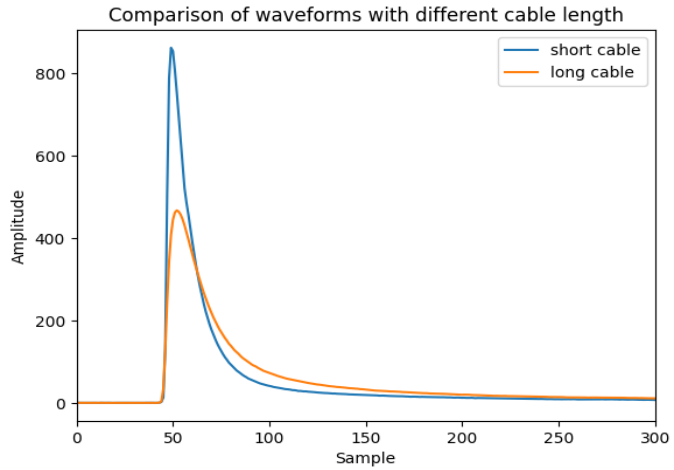
Coordinates of the detector and collimator

- Collimator position =(5908.0, −7311.329, −200.0)mm
- Detector position=(6411.13, −8344.94, −200.0) mm
- Distance ≈ 1150 mm

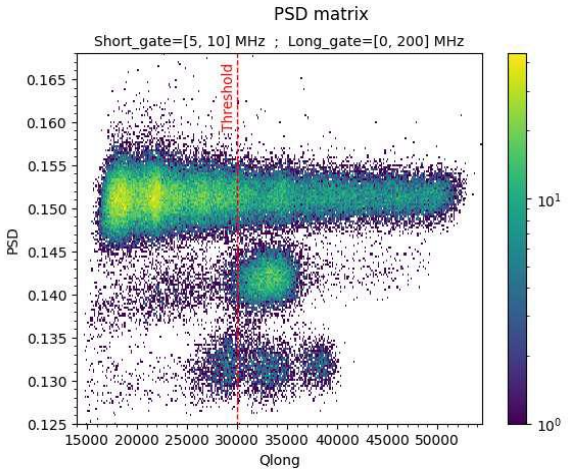


Effect of long cable and e.m. noise on particle discrimination

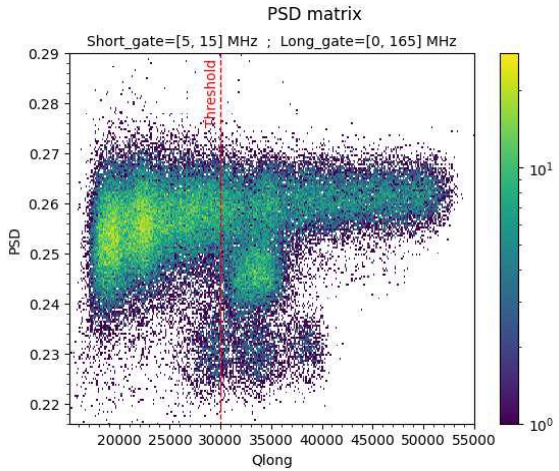
- Long cables smooth the signals, potentially compromising the particle discrimination.
- Tests with 100 m long cable has been performed on intrinsic activity measurements -> No significant degradation has been found in terms of FOM
- Poissonian noise added offline to 2.5 MeV neutron measurement (to simulate e.m. noise) -> **e. m. noise can definitely affect the particle discrimination!**



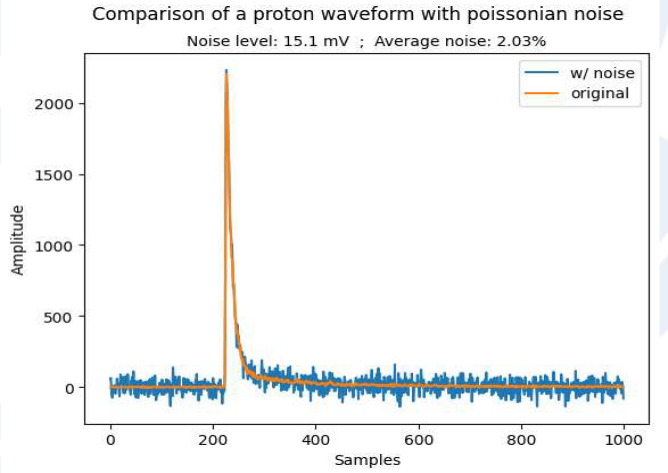
Example of waveforms recorded with short and long cables.



Without poissonian noise

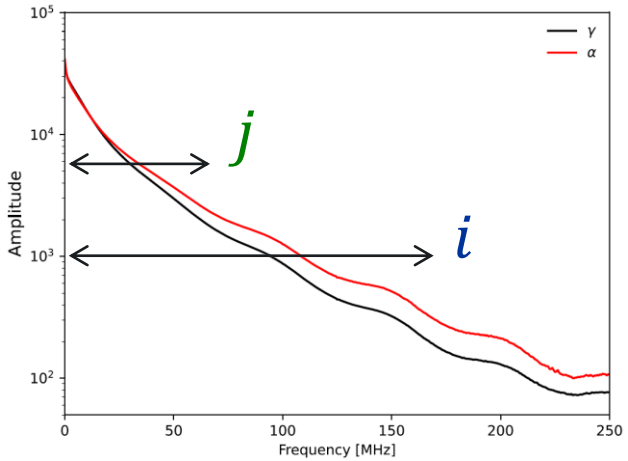


With poissonian noise



Example of waveforms with and without poissonian noise.

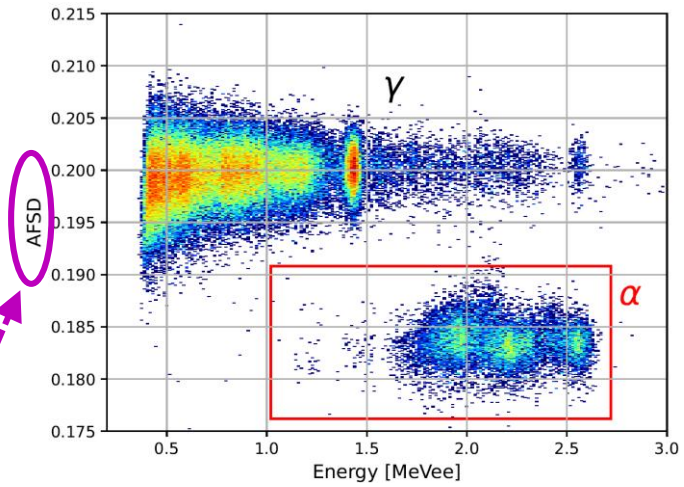
- New method based on **Fast Fourier Transforms FFT** has been developed and tested with **intrinsic activity** measurements (**γ and α events**) of the $LaCl_3$ crystal itself.



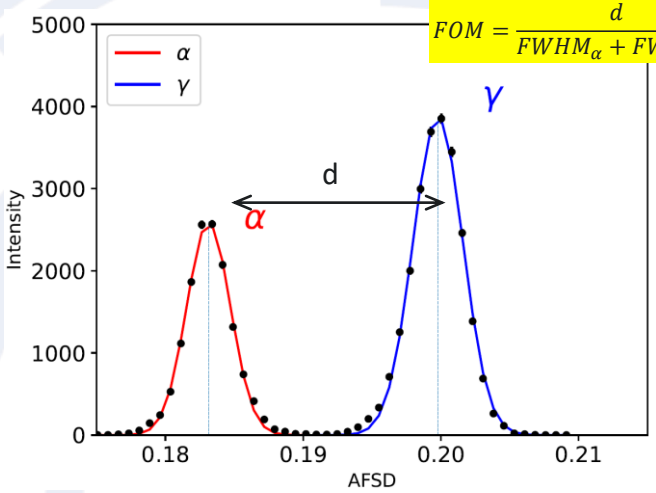
Waveforms in freq. domain.

$$y[k] = \sum_{n=0}^{N-1} e^{-2\pi i \frac{k_n}{N}} x[n]$$

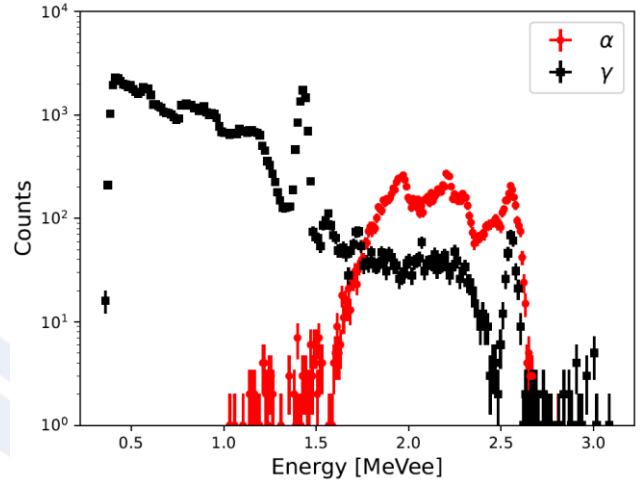
$$AFSD = \frac{\sum_{n=0}^{j} ||y[k_n||}{\sum_{n=0}^{i} ||y[k_n||}$$



AFSD matrix obtained with the FFT method on the intrinsic activity measurement of the $LaCl_3$ scintillator.



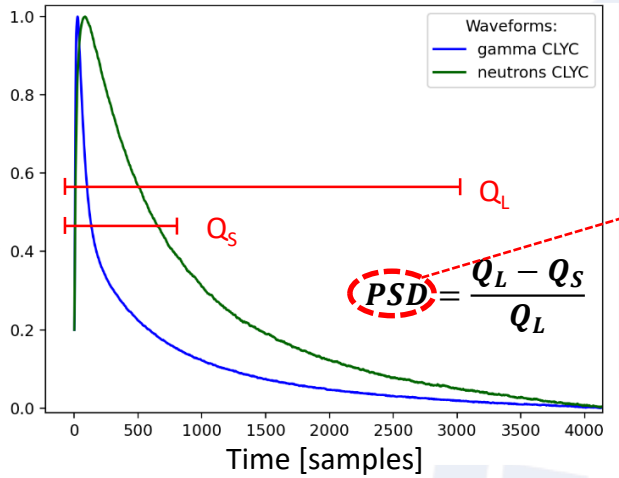
FOM: AFSD spectrum obtained as the projection of the 2D scatterplot of the AFSD values .



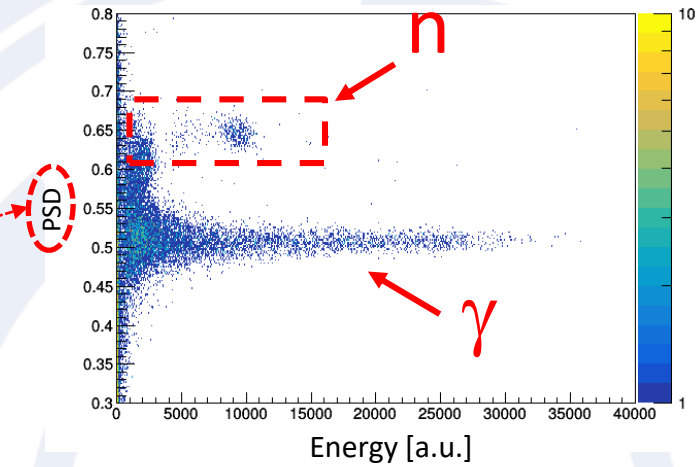
D Rigamonti et al 2025 Meas. Sci. Technol. 36 015907
D Rigamonti et al 2026 Meas. Sci. Technol. 37 065501

C7LYC scintillators and standard PSD

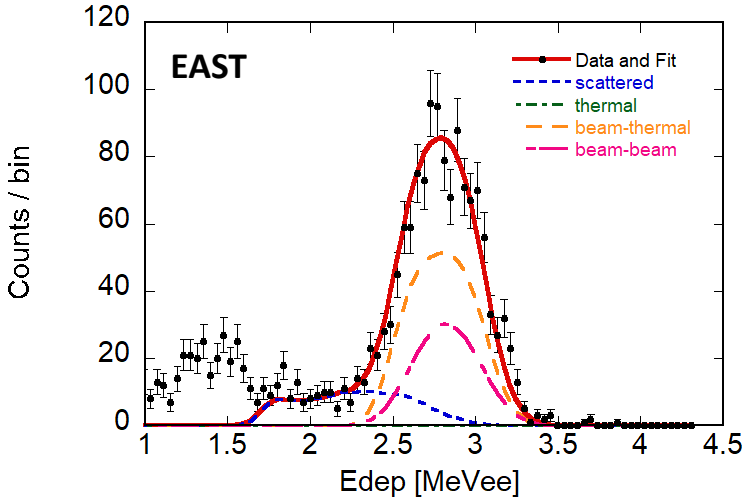
- C7LYC (Cs2LiYCl6 :Ce) with 99% of 7Li
- Good energy resolution (6% @ 137Cs line)
- **Excellent n/γ separation with standard pulse shape discrimination (PSD) algorithm**
- **Already demonstrated working on tokamaks (EAST, ASDEXu) -> Neutron emission components resolved**
- **Scintillation time very slow - > Max a few tens of kHz**



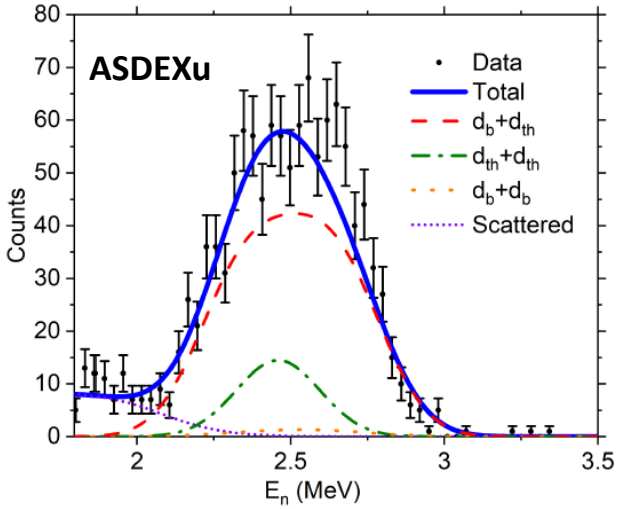
Example of waveforms related to neutron and gamma events collected with a CLYC detector



Example of PSD matrix obtained with a CLYC detector in a mixed n and γ flux.



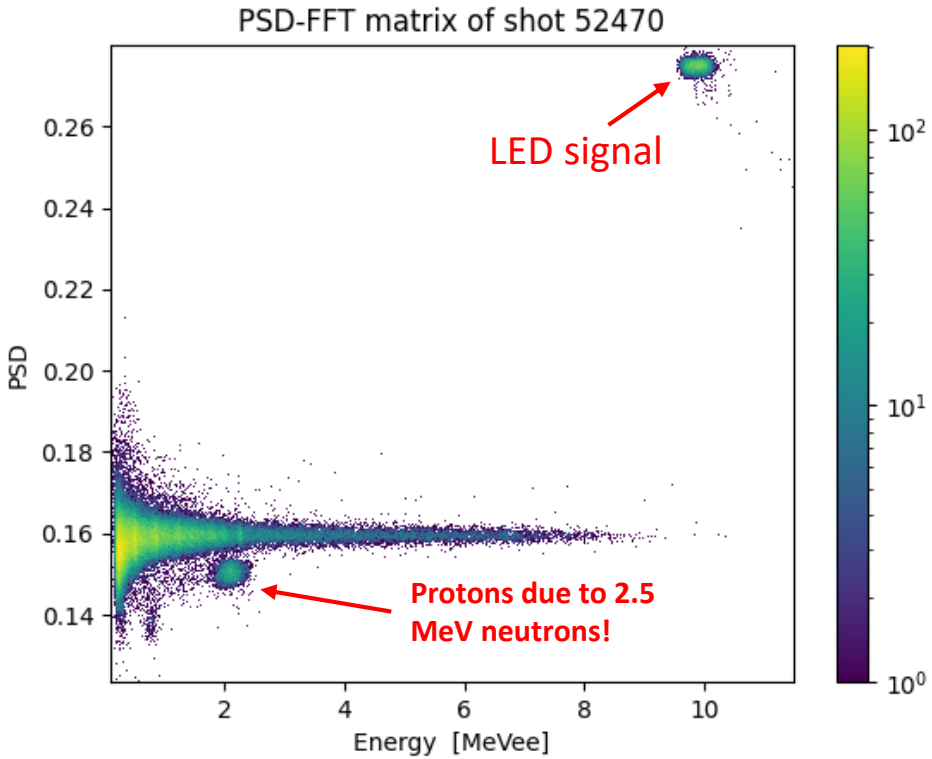
Measured 2.5 MeV neutron spectrum at EAST with CLYC detector.



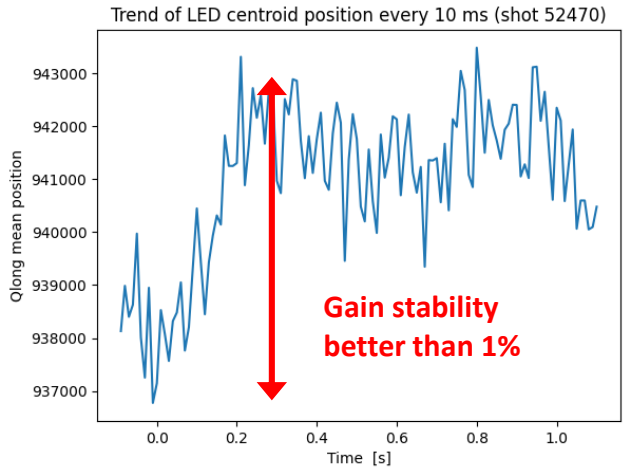
Measured 2.5 MeV neutron spectrum at ASDEXu with CLYC detector.

D. Rigamonti et al 2019 JINST 14 C09025
M. Nocente et al. Rev. Sci. Instrum. 95, 083501 (2024)

First neutron measurement at MASTu



"PSD" matrix for shot 52470



Time trace of the LED pulses during shot 52470

